RESEARCH ARTICLE

Earlobe Electrical Signatures: A Non-Invasive Biophysical Tool for Rapid Quantification of Human Systemic Information

Yanyou Wu[1,2,*]

[1] State Key Laboratory of Environmental Geochemistry, Institute of Geochemistry, Chinese Academy of Sciences, Guiyang 550081, China
[2] School of Agricultural Engineering, Jiangsu University, Zhenjiang 212013, China

Abstract

Conventional physiological assessment methods are limited by invasiveness, single-index detection, and the lack of objective biophysical indicators integrating Traditional Chinese Medicine (TCM) and Western medicine principles. This study presents a non-invasive biophysical method for rapid quantification of human systemic physiological information via earlobe electrical parameters, and establishes pressure-dependent biophysical models for these parameters based on thermodynamic and electrophysiological principles. Earlobe capacitance, resistance, impedance, capacitive reactance, and inductive reactance were measured at 9 gradient pressure levels (0.5–6 N) using a portable detection system with a parallel-plate capacitor sensor and pressure-regulated clamp. The Gibbs free energy and Nernst equations were applied to construct a linear model for capacitance and nonlinear exponential decrease models for the other parameters, from which indicators of energy conversion, substance transfer/transport, and metabolic capacity were derived. The models achieved high fitting accuracy ($R^2 > 0.97$), and the three healthy subjects exhibited similar transfer numbers of dielectric substances and similar water transport efficiency. The $\mathrm{RG}_{Xc\text{-}Xl}$ ratio, proposed as a candidate biomarker for TCM Yin-Yang balance, was close to unity (0.986–1.036) in all participants, consistent with a balanced physiological status; total detection time (excluding resting) was < 3 min. These results suggest that earlobe electrical parameters may serve as a sensitive peripheral signature of systemic physiological function, offering a portable tool for large-scale health screening and early physiological assessment. As a preliminary feasibility study of three healthy participants, these findings require confirmation in larger, more diverse cohorts and independent clinical validation.

Keywords: earlobe electrical parameters, non-invasive biophysical detection, pressure-dependent model, biophysical modeling, Yin-Yang balance.

Submitted: 14 April 2026
Revised: 14 June 2026
Accepted: 23 October 2026
Published: 27 November 2026

Vol. 1, **No.** 2, 2026.
10.62762/FBSP.2026.693858

***Corresponding author:**
✉ Yanyou Wu
wuyanyou@mail.gyig.ac.cn

Citation
Wu, Y. (2026). Earlobe Electrical Signatures: A Non-Invasive Biophysical Tool for Rapid Quantification of Human Systemic Information. *Frontiers in Biomedical Signal Processing*, 1(2), 105–122.

© 2026 by the Author. Published by Institute of Central Computation and Knowledge. This is an open access article under the CC BY license (https://creativecommons.org/licenses/by/4.0/).

1 Introduction

Non-invasive biophysical detection of human physiological information is a core research direction in medical physics and biomedical engineering. Non-invasive sensing is already used to quantify metabolism and biophysical transport in cells and tissues and to support clinical diagnosis [1, 2], and it is relevant to public health screening, sub-health identification, and personalized health management. Traditional physiological assessment methods (e.g., blood sampling, imaging) suffer from invasiveness, high cost, and single-index limitation, making them unsuitable for regular and large-scale application. Meanwhile, the integration of TCM holistic diagnosis (e.g., Yin-Yang balance) with Western medicine quantitative biophysical detection remains a challenge, due to the lack of mechanistically defined biophysical models and objective quantifiable indicators.

In plants, photosynthesis is carried out via leaves to fulfill autotrophic functions. Among these, biophysical functions are determined by the energy storage and conversion capacities of the electrical components within their cells [3]. In contrast, humans, as heterotrophs, rely on eight major systems–musculoskeletal, nervous, endocrine, circulatory, respiratory, digestive, urinary, and reproductive systems–to coordinate complex life activities. The diversity of cellular structures and functions across organs makes it challenging to noninvasively obtain selective energy storage and conversion information from specific tissues to characterize physiological function, organ status, and overall health.

TCM theory regards the ear as a window for human physiological information, reflecting systemic visceral and meridian functions. The earlobe is a cartilage-free structure composed of adipose and fibrous tissue located beneath the helix [4], and it is a routine site for capillary blood sampling [5]. Ear blood tests are routinely used to assess metabolic and organ functions via glucose, lipid, liver, renal, and electrolyte analyses.

The most fundamental difference between human earlobe cells and plant leaf cells is the absence of cell walls and the inability to perform photosynthetic autotrophy. Leaves consist of epidermis, mesophyll (including palisade and spongy tissues), and veins. The epidermis is covered with stomata, which are typically composed of two kidney-shaped guard cells. Earlobe tissue is composed of adipose and connective tissues. Adipose tissue is composed of adipocytes containing triglyceride reservoirs, whereas connective tissue consists of cells and an abundant intercellular matrix. The intercellular matrix of connective tissue includes liquid, colloidal, or solid matrices; filamentous fibers; and continuously renewed tissue fluid [6]. Because of the heterogeneous structure of plant leaves and the presence of cell walls in leaf cells, coupled with the fact that leaf assimilation is a critical prerequisite for plant physiological functions, it is challenging to obtain resting electrical parameters that are unrelated to photosynthetic capacity. However, earlobe cells exhibit excellent homogeneity, lack cell walls, perform heterotrophic functions, and possess unique compositional characteristics, enabling the acquisition of electrical parameters (e.g., average resting capacitance, resistance, inductive reactance, capacitive reactance, and impedance) and metabolic capabilities based on heterotrophic functions.

Cells and organelles are enclosed by a cell membrane primarily composed of lipids (∼50%), proteins (∼40%), and carbohydrates (2–10%). The phospholipid bilayer forms the membrane scaffold, appearing under electron microscopy as three layers: 2.5 nm electron-dense bands (hydrophilic regions) on both sides and a 2.5 nm transparent band (hydrophobic region) in between [7]. This structure allows cells and organelles to be modeled as concentric spherical capacitors with membrane proteins, conferring both capacitive and inductive properties [8].

The electrical components within cells absorb, store, and convert energy, resulting in alterations in both substance and energy metabolism [9]. The Gibbs free energy equation and Nernst equation effectively characterize the conversion of diverse energy forms and the transformation of energy into chemical energy within a system. Therefore, measuring earlobe electrical parameters (which mirror human physiological information) and analyzing earlobe cellular electrical behavior and biophysical properties via these equations can potentially reflect human physiological functions (especially heterotrophic substance metabolism capacity), visceral/organ functions, and health status; the thermodynamic basis of such bioenergetic analysis is established [10]. This provides fundamental data for disease diagnosis, health evaluation, and specialized personnel recruitment (e.g., athletes, astronauts) while offering a quantitative foundation for TCM theories such as Yin-Yang balance, energy conversion, and substance transfer/transport, facilitating the integration of

traditional and modern medicine.

This study employed plant health and metabolic activity measurement methods, integrating thermodynamic and electrophysiological principles and biophysical modeling technology to establish a non-invasive rapid acquisition technology system for human biophysical information based on earlobe electrical parameters [3]. The specific objectives are as follows: (1) Develop a non-invasive method to measure earlobe electrical parameters under varying pressures; (2) Construct pressure-dependent models of electrical parameters using thermodynamic and electrophysiological principles and biophysical modeling technology; (3) Establish calculation methods for key biophysical indicators (e.g., unit resting capacitance/resistance, energy conversion, substance transfer/transport, and metabolic capacity).

2 Materials and Methods

2.1 Study Participants

Three healthy adult males (aged 63 ± 0.1 years, mean $\pm$ SD) with no history of chronic diseases were recruited. Informed consent was obtained from all participants in the study. The study protocol was conducted in accordance with the ethical principles of minimal risk research for human subjects, with no invasive procedures, no manipulation of physiological status, and no potential physical/psychological risks. All experimental data were anonymized for analysis to ensure participant privacy. Owing to the small sample size, the present findings should be regarded as preliminary and should not be generalized to broader populations without further validation.

2.2 Electrophysiological Signal Recording

Earlobe electrophysiological signals were recorded using a portable Plant Life Analyzer (Jiangsu Zhong-tian Smart Sense Life Data Co., Ltd., Zhenjiang, China; Figure 1), equipped with a custom parallel-plate capacitor sensor (effective diameter $D = 0.7$ cm), an LCR meter (GWINSTEK, Suzhou, China), and a pressure-regulated clamp (range: 0.5–6 N, precision: ± 0.01 N). Measurements were conducted in parallel mode with a test voltage of 1.5 V and a frequency of 3 kHz.

2.3 Experimental Protocol

The participants rested in a quiet room for 20 minutes to stabilize their physiological status. The parallel-plate capacitor sensor was clamped gently at the center of the earlobe. Electrical parameters

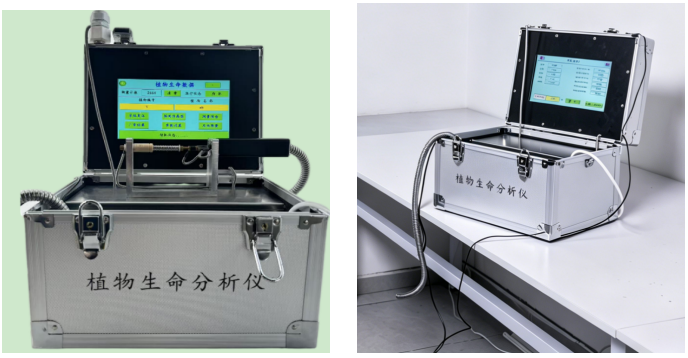


Figure 1. Portable Plant Life Analyzer (Jiangsu Zhong-tian Smart Sense Life Data Co., Ltd., Zhenjiang, China).

(capacitance C_p, resistance R, impedance Z, capacitive reactance Xc, and inductive reactance Xl) were measured at nine randomly selected pressure levels in the parallel mode. A steady-state pressure duration of 10 s was maintained at each pressure level, with continuous data acquisition performed to ensure measurement stability. Across all nine pressure levels, a total of $n = 90$ electrical parameter records were aggregated from each participant, comprising ten repeated measurements per pressure level to support subsequent model fitting.

2.4 Biophysical Model Construction and Indicator Calculation

2.4.1 *Pressure-Dependent Biophysical Models of Electrical Parameters*

The core of this study is the construction of pressure-dependent biophysical models for earlobe electrical parameters based on the Gibbs free energy equation (for energy conversion) and Nernst equation (for ion concentration gradient changes). Separate linear and nonlinear exponential models were established for capacitance and other electrical parameters, respectively.

The proposed pressure-dependent models rest on several simplifying assumptions. First, energy conservation is assumed: the mechanical work performed by the clamping force is converted into the electrostatic energy stored by the earlobe cells, which are idealized as concentric-sphere capacitors under a constant test voltage; clamping is treated as isothermal, and the Helmholtz free energy change of the earlobe system is assumed to be independent of the clamping force. Second, the capacitance model assumes a linear relationship between the effective thickness (d) of the compressed earlobe and the applied pressure within the tested range. Third, the resistance, impedance, capacitive reactance,

and inductive reactance models assume that the transmembrane transport of ions and electric dipoles follows the Nernst equation, and that the converted pressure work is linearly related to the electromotive force. Fourth, the earlobe tissue is treated as electrically homogeneous within the measurement window, and resting (near-zero-pressure) parameters are extrapolated from the fitted models. It should be emphasized that, although the mathematical forms are derived from thermodynamic and electrophysiological principles, they also involve empirical curve fitting to the measured data; therefore, their physical interpretation should be distinguished from purely empirical fitting, and the underlying assumptions require further experimental validation across broader pressure and population ranges.

(1) Capacitance Model

According to the classical definitions of thermodynamic potentials, $G = H - TS_{\text{en}}$ and $H = U_{\text{in}} + PV$; hence the Gibbs free energy can be written as $G = A + PV$, where $A = U_{\text{in}} - TS_{\text{en}}$ is the Helmholtz free energy. Taking the unclamped earlobe (zero applied pressure) as the reference state and assuming that clamping is isothermal, the change in the Gibbs free energy of the clamped earlobe system caused by the clamping force is

$$\Delta G = \Delta A + PV \tag{1}$$

where ΔG is the change in Gibbs free energy (J), $\Delta A = \Delta U_{\text{in}} - T\Delta S_{\text{en}}$ is the change in Helmholtz free energy of the earlobe system (J), which is assumed to be independent of the clamping force within the tested range, ΔU_{in} is the change in internal energy (J), T is the thermodynamic temperature (K), ΔS_{en} is the entropy change ($\text{J}\cdot\text{K}^{-1}$), P is the pressure intensity of the earlobe (Pa), and V is the volume of the clamped part of the earlobe (m^3), treated as constant. P can be computed using the pressure-intensity formula:

$$P = \frac{F}{S} \tag{2}$$

where F symbolizes the clamping force (N), and S represents the effective area of the electrode plate (m^2). Earlobe cells can be regarded as concentric-sphere capacitors, and the energy of the capacitor is expressed as

$$W = \frac{1}{2}U^2 C_p \tag{3}$$

where W is the capacitor energy (J), U is the test voltage (V), and C_p is the physiological capacitance (pF).

Based on the principle of energy conservation, the capacitor energy is equivalent to the work converted from the Gibbs free energy, that is, $W = \Delta G$. The relationship model between the earlobe capacitance C_p and clamping force (F) is derived as

$$C_p = \frac{2\Delta A}{U^2} + \frac{2V}{SU^2}F \tag{4}$$

It is hypothesized that d represents the earlobe-specific effective thickness; thus, $d = V/S$, and Equation (4) is transformed into Equation (5):

$$C_p = \frac{2\Delta A}{U^2} + \frac{2d}{U^2}F \tag{5}$$

Let $x_0 = 2\Delta A/U^2$ and $h = 2d/U^2$; Equation (5) is further transformed into Equation (6):

$$C_p = x_0 + hF \tag{6}$$

Equation (6) is a linear pressure-dependent capacitance model, where x_0 and h are the model biophysical parameters. As $h = 2d/U^2$, the earlobe specific effective thickness (d) (a key tissue biophysical characteristic) can be calculated as:

$$d = \frac{U^2 h}{2} \tag{7}$$

(2) Resistance / Impedance / Capacitive Reactance / Inductive Reactance Models

The Nernst equation can be used to describe the changes in the concentration of ions, ion groups, and electric dipoles inside and outside the cell membrane. The resistance (R) depends on the concentration of ions inside and outside the membrane and follows the Nernst equation, which is expressed as follows:

$$E - E^0 = \frac{R_{\text{g}}T}{n_R F_0}\ln\frac{C_i}{C_o} \tag{8}$$

where E is the electromotive force (V), E^0 is the standard electromotive force (V), R_{g} is the gas constant ($8.314\ \text{J}\cdot\text{K}^{-1}\cdot\text{mol}^{-1}$), T is the thermodynamic temperature (K), C_i is the concentration of electrolytes that respond to R inside the cell membrane ($\text{mol}\cdot\text{L}^{-1}$), C_o is the concentration of electrolytes that respond to R outside the cell membrane ($\text{mol}\cdot\text{L}^{-1}$), F_0 is the Faraday constant ($9.65 \times 10^4\ \text{C}\cdot\text{mol}^{-1}$), and n_R is the charge number of the transferred electrolyte ions (dimensionless).

The internal energy of the electromotive force can be converted into pressure work, and they have a direct relationship, $PV = aE$, that is,

$$PV = aE = aE^0 + \frac{aR_{\text{g}}T}{n_R F_0}\ln\frac{C_i}{C_o} \tag{9}$$

where a is the transfer coefficient from electromotive force to energy.

For the earlobe cells, the sum of C_o and C_i is certain. C_i is directly proportional to the conductivity of the electrolytes that respond to R, and the conductivity is the reciprocal of R. Hence, C_i/C_o can be expressed as $\frac{C_i}{C_o} = \frac{f_0/R}{C_T - f_0/R} = \frac{f_0}{C_T R - f_0}$, where f_0 is the transfer coefficient between C_i and R, and $C_T = C_i + C_o$. Therefore, Equation (9) was transformed into Equation (10):

$$\frac{V}{S}F = aE^0 - \frac{aR_gT}{n_RF_0}\ln\frac{C_TR - f_0}{f_0} \tag{10}$$

Equation (10) was rewritten as:

$$\frac{aR_gT}{n_RF_0}\ln\frac{C_TR - f_0}{f_0} = aE^0 - \frac{V}{S}F \tag{11}$$

Equation (11) can be rewritten as Equation (12):

$$\ln\frac{C_TR - f_0}{f_0} = \frac{n_RF_0E^0}{R_gT} - \frac{Vn_RF_0}{SaR_gT}F \tag{12}$$

Taking the exponents of both sides of Equation (12):

$$\frac{C_TR - f_0}{f_0} = e^{\frac{n_RF_0E^0}{R_gT}}e^{-\frac{Vn_RF_0}{SaR_gT}F} \tag{13}$$

Further:

$$R = \frac{f_0}{C_T} + \frac{f_0}{C_T}e^{\frac{n_RF_0E^0}{R_gT}}e^{-\frac{Vn_RF_0}{SaR_gT}F} \tag{14}$$

Because $d = V/S$, Equation (14) was transformed into:

$$R = \frac{f_0}{C_T} + \frac{f_0}{C_T}e^{\frac{n_RF_0E^0}{R_gT}}e^{-\frac{dn_RF_0}{aR_gT}F} \tag{15}$$

For the same test in the same environment, d, a, E^0, R_g, T, n_R, F_0, C_T, and f_0 of Eq. (15) are constant. Let $y_1 = f_0/C_T$, $k_1 = \frac{f_0}{C_T}e^{\frac{n_RF_0E^0}{R_gT}}$, and $b_1 = \frac{dn_RF_0}{aR_gT}$; the intrinsic mechanistic relationship between resistance (R) and F conforms to a nonlinear exponential decrease pressure-dependent resistance model, which is presented as follows:

$$R = y_1 + k_1e^{-b_1F} \tag{16}$$

where y_1, k_1, and b_1 are the model fitting biophysical parameters, reflecting the intrinsic electrical characteristics of earlobe tissue.

Following the same biophysical derivation principle, nonlinear exponential decrease pressure-dependent models for Z, Xc, and Xl were derived as follows:

$$Z = y_2 + k_2e^{-b_2F} \tag{17}$$

$$Xc = y_3 + k_3e^{-b_3F} \tag{18}$$

$$Xl = y_4 + k_4e^{-b_4F} \tag{19}$$

where y_2 (y_3/y_4), k_2 (k_3/k_4), and b_2 (b_3/b_4) are the model fitting parameters for each electrical parameter.

2.4.2 Calculation of Resting Electrical Parameters

Resting electrical parameters (at zero clamping pressure, $F = 0$) are the intrinsic biophysical characteristics of earlobe tissue, and were calculated directly from the established pressure-dependent models.

According to Eq. (16), when $F = 0$, the earlobe resting resistance (IR) can be obtained as

$$\mathrm{IR} = y_1 + k_1 \tag{20}$$

Similar to IR, when $F = 0$, the earlobe resting impedance (IZ), earlobe resting capacitive reactance (IXc), and earlobe resting inductive reactance (IXl) can be calculated as

$$\mathrm{IZ} = y_2 + k_2 \tag{21}$$

$$\mathrm{IXc} = y_3 + k_3 \tag{22}$$

$$\mathrm{IXl} = y_4 + k_4 \tag{23}$$

The earlobe resting capacitance (ICP) could also be obtained:

$$\mathrm{ICP} = \frac{1}{2\pi f \times \mathrm{IXc}} \tag{24}$$

where $\pi = 3.1416$, f is the frequency, and IXc is the earlobe resting capacitive reactance.

Given that the measurement is performed in parallel mode, based on electrical principles, the unit resting resistance $\mathrm{IR}_U = \mathrm{IR} \times d$, unit resting impedance $\mathrm{IZ}_U = \mathrm{IZ} \times d$, unit resting capacitive reactance $\mathrm{IXc}_U = \mathrm{IXc} \times d$, unit resting inductive reactance $\mathrm{IXl}_U = \mathrm{IXl} \times d$, and unit resting capacitance $\mathrm{ICP}_U = \mathrm{ICP}/d$.

2.4.3 Calculation of Key Biophysical Indicators

Based on the resting electrical parameters and pressure-dependent model fitting parameters, five categories of core biophysical indicators were calculated to characterize human systemic physiological function, including energy conversion capacity, intracellular water transfer/transport capacity, intracellular nutrient transfer/transport capacity, dielectric substance transfer/transport capacity, and metabolic capacity. All calculation formulas were derived based on thermodynamic, electrophysiological and biophysical principles, with the core formulas presented as follows:

(1) Energy conversion capacity

The energy conversion capabilities of earlobe cells include the resistance-based unit internal energy $\Delta G_{R\text{-}U}$, resistance-based internal energy ΔG_R, capacitive reactance-based unit internal energy $\Delta G_{Xc\text{-}U}$, capacitive reactance-based internal energy ΔG_{Xc}, inductive reactance-based unit internal energy $\Delta G_{Xl\text{-}U}$, inductive reactance-based internal energy ΔG_{Xl}, impedance-based unit internal energy $\Delta G_{Z\text{-}U}$, impedance-based internal energy ΔG_Z, average unit internal energy ΔG_U, and capacitive reactance internal energy/inductive reactance internal energy $\mathrm{RG}_{Xc\text{-}Xl}$.

Based on Equations (15) and (16), the resistance-based unit internal energy $\Delta G_{R\text{-}U}$ was computed:

$$\Delta G_{R\text{-}U} = \frac{aE^0}{d} = \frac{\ln k_1 - \ln y_1}{b_1} \tag{25}$$

Analogous to the derived formula for $\Delta G_{R\text{-}U}$, the capacitive reactance-based unit internal energy $\Delta G_{Xc\text{-}U}$, inductive reactance-based unit internal energy $\Delta G_{Xl\text{-}U}$, and impedance-based unit internal energy $\Delta G_{Z\text{-}U}$ were derived:

$$\Delta G_{Xc\text{-}U} = \frac{\ln k_3 - \ln y_3}{b_3} \tag{26}$$

$$\Delta G_{Xl\text{-}U} = \frac{\ln k_4 - \ln y_4}{b_4} \tag{27}$$

$$\Delta G_{Z\text{-}U} = \frac{\ln k_2 - \ln y_2}{b_2} \tag{28}$$

Consequently, the resistance-based internal energy ΔG_R, capacitive reactance-based internal energy ΔG_{Xc}, inductive reactance-based internal energy ΔG_{Xl}, and impedance-based internal energy ΔG_Z are computed as follows:

$$\Delta G_R = \Delta G_{R\text{-}U} \times d \tag{29}$$

$$\Delta G_{Xc} = \Delta G_{Xc\text{-}U} \times d \tag{30}$$

$$\Delta G_{Xl} = \Delta G_{Xl\text{-}U} \times d \tag{31}$$

$$\Delta G_Z = \Delta G_{Z\text{-}U} \times d \tag{32}$$

The computational approach for the average unit internal energy ΔG_U is presented as follows:

$$\Delta G_U = \frac{\Delta G_{R\text{-}U} + \Delta G_{Z\text{-}U} + \Delta G_{Xc\text{-}U} + \Delta G_{Xl\text{-}U}}{4} \tag{33}$$

The calculation method for the capacitive reactance internal energy/inductive reactance internal energy $\mathrm{RG}_{Xc\text{-}Xl}$ is as follows:

$$\mathrm{RG}_{Xc\text{-}Xl} = \frac{\Delta G_{Xc\text{-}U}}{\Delta G_{Xl\text{-}U}} \tag{34}$$

(2) Intracellular water transfer/transport capacity

The intracellular water transport capacity of earlobe cells comprises four parameters: the intracellular water-holding capacity (IWHC), the intracellular water transfer/transport efficiency (IWTTE), the intracellular water-holding time (IWHT), and the intracellular water transfer/transport rate (IWTTR).

The earlobe cells can be regarded as a spherical structure, and the capacitance C_S can be calculated using the formula for concentric spherical capacitors:

$$C_S = \frac{4\pi\varepsilon r_1 r_2}{r_2 - r_1} \tag{35}$$

where $\pi = 3.1416$, C_S is the capacitance of the concentric spherical capacitor (pF), ε is the dielectric constant of the electrolyte, r_1 is the inner-sphere radius (m), and r_2 is the outer-sphere radius (m). For an earlobe cell, $r_2 - r_1$ is the thickness of the cell membrane. Because $r_1 \approx r_2$, and both ε and the membrane thickness are constant, the cell volume (V_C) is directly proportional to $\sqrt{C_S^3}$.

The main component of the earlobe cell is water (approximately 75%). Therefore, $\sqrt{C_S^3}$ represents the water-holding capacity of earlobe cells. The intracellular water-holding capacity (IWHC) of earlobe cells was obtained according to Equation (36):

$$\mathrm{IWHC} = \sqrt{\mathrm{ICP}^3} \tag{36}$$

Therefore, the intracellular water transfer/transport efficiency (IWTTE) is represented by Equation (37):

$$\mathrm{IWTTE} = \frac{d}{\mathrm{IWHC}} \tag{37}$$

According to Ohm's law, $I_Z = U/Z$, where I_Z is the physiological current (A). At the same time, the current is equal to the product of the capacitance and the differential of the voltage in time, as shown in Equation (38):

$$I_Z\left(i(t)\right) = \mathrm{ICP} \times \frac{\mathrm{d}u(t)}{\mathrm{d}t} \tag{38}$$

where $i(t)$ denotes the instantaneous current in amperes (A), a function of time t; $u(t)$ represents

the instantaneous voltage across the capacitor in volts (V), also a function of time t; and $\mathrm{d}u(t)/\mathrm{d}t$ is the first derivative of voltage $u(t)$ with respect to time t, indicating the rate of change in voltage over time.

After the integral transformation, the current time is the product of ICP and IZ. Therefore, the intracellular water-holding time (IWHT) is represented by Equation (39):

$$\mathrm{IWHT} = \mathrm{ICP} \times \mathrm{IZ} \tag{39}$$

Accordingly, the intracellular water transfer/transport rate (IWTTR) is calculated using Equation (40):

$$\mathrm{IWTTR} = \frac{\mathrm{IWHC}}{\mathrm{IWHT}} \tag{40}$$

(3) Intracellular nutrient transfer/transport capacity

The intracellular nutrient transfer/transport capacity of earlobe cells includes the intracellular nutrient transfer/transport rate (INTTR), active transfer/transport unit flow (UATTF), intracellular nutrient active transfer/transport capacity (NATTC), intracellular nutrient passive transfer/transport unit flow (UPTTF), intracellular nutrient passive transfer/transport capacity (NPTTC), intracellular nutrient transfer/transport unit flow (UNTTF), intracellular nutrient transfer/transport capacity (NTTC), intracellular nutrient transfer/transport efficiency (INTTE), and ratio of intracellular active to passive transfer/transport capacity (RAP).

Given that nutrients exhibit water solubility, the intracellular water transfer/transport rate (IWTTR) and intracellular nutrient transfer/transport rate (INTTR) were regarded as equivalent, as delineated in Equation (41):

$$\mathrm{INTTR} = \mathrm{IWTTR} \tag{41}$$

Earlobe cells possess electrical characteristics of low capacitance (C) and high resistance/impedance (R/Z). It can be hypothesized that these cells are connected in parallel. In accordance with the calculation formula for the resistance in a parallel circuit, the earlobe resistance R can be computed using the following formula:

$$\frac{1}{R} = \frac{1}{R_1} + \frac{1}{R_2} + \frac{1}{R_3} + \cdots + \frac{1}{R_n} \tag{42}$$

where $R_1, R_2, R_3, \ldots, R_n$ denote the resistances of the individual unit cell membranes.

Assuming that the resistance of each unit cell membrane is equivalent, that is, $R_1 = R_2 = R_3 = \cdots = R_n = R_0$, the earlobe resistance (R) can be computed using the formula:

$$\frac{1}{R} = \frac{n}{R_0} \tag{43}$$

Here, n can be defined as the quantity of proteins and lipids that induce resistance in biological tissues.

Based on the calculation formula for the capacitive reactance in a parallel circuit, the earlobe capacitive reactance Xc can be computed using the following formula:

$$\frac{1}{Xc} = \frac{1}{Xc_1} + \frac{1}{Xc_2} + \frac{1}{Xc_3} + \cdots + \frac{1}{Xc_p} \tag{44}$$

where $Xc_1, Xc_2, Xc_3, \ldots, Xc_p$ are the capacitive reactances of each unit cell membrane.

Assuming that the capacitive reactance of each unit cell membrane is equivalent, namely $Xc_1 = Xc_2 = Xc_3 = \cdots = Xc_p = Xc_0$, the earlobe capacitive reactance can be computed using the subsequent formula:

$$\frac{1}{Xc} = \frac{p}{Xc_0} \tag{45}$$

In this context, p can be defined as the number of proteins, especially surface proteins (peripheral proteins), that contribute to the capacitive reactance of biological tissues.

The formula for calculating the inductive reactance of the earlobe (Xl) is:

$$\frac{1}{Xl} = \frac{1}{Xl_1} + \frac{1}{Xl_2} + \frac{1}{Xl_3} + \cdots + \frac{1}{Xl_q} \tag{46}$$

where $Xl_1, Xl_2, Xl_3, \ldots, Xl_q$ denote the inductive reactances of each unit cell membrane.

Assuming that the inductive reactance of each unit cell membrane is equivalent, namely $Xl_1 = Xl_2 = Xl_3 = \cdots = Xl_q = Xl_0$, the formula for calculating the earlobe inductive reactance is

$$\frac{1}{Xl} = \frac{q}{Xl_0} \tag{47}$$

Herein, q can be defined as the quantity of protein-binding proteins (intrinsic proteins), especially transport proteins, that induce tissue reactance.

The passive transfer/transport capacity of nutrients is determined by the ratio of the cellular substance

transfer/transport capacity mediated by surface proteins (peripheral proteins) to the total cellular substance transfer/transport capacity, while the active transfer/transport capacity of nutrients is determined by the ratio of the cellular substance transfer/transport capacity mediated by binding proteins to the total cellular substance transfer/transport capacity.

The active transfer/transport unit flow (UATTF) was computed using the following formula:

$$\begin{aligned} \mathrm{UATTF} &= \frac{\mathrm{IXl}^{-1}}{\mathrm{IR}^{-1}} = \frac{q/\mathrm{IXl}_0}{n/\mathrm{IR}_0} \\ &= \frac{q}{n}\frac{\mathrm{IR}_0}{\mathrm{IXl}_0} = \frac{\mathrm{IR}}{\mathrm{IXl}} \end{aligned} \tag{48}$$

Meanwhile, given that $\frac{q\,\mathrm{IR}_0}{n\,\mathrm{IXl}_0}$ is constant for the same measurement sample, the formula for calculating the intracellular nutrient active transfer/transport capacity (NATTC) is as follows:

$$\mathrm{NATTC} = \mathrm{UATTF} \times \mathrm{INTTR} \tag{49}$$

The intracellular nutrient passive transfer/transport unit flow (UPTTF) was computed using the following formula:

$$\begin{aligned} \mathrm{UPTTF} &= \frac{\mathrm{IXc}^{-1}}{\mathrm{IR}^{-1}} = \frac{p/\mathrm{IXc}_0}{n/\mathrm{IR}_0} \\ &= \frac{p}{n}\frac{\mathrm{IR}_0}{\mathrm{IXc}_0} = \frac{\mathrm{IR}}{\mathrm{IXc}} \end{aligned} \tag{50}$$

Similarly, given that $\frac{p\,\mathrm{IR}_0}{n\,\mathrm{IXc}_0}$ is constant for the same measurement sample, the formula for calculating the intracellular nutrient passive transfer/transport capacity (NPTTC) is as follows:

$$\mathrm{NPTTC} = \mathrm{UPTTF} \times \mathrm{INTTR} \tag{51}$$

Therefore, the intracellular nutrient transfer/transport unit flow (UNTTF) was computed using the following formula:

$$\mathrm{UNTTF} = \mathrm{UATTF} + \mathrm{UPTTF} = \frac{\mathrm{IR}}{\mathrm{IXc}} + \frac{\mathrm{IR}}{\mathrm{IXl}} \tag{52}$$

The formula for calculating intracellular nutrient transfer/transport capacity (NTTC) is as follows:

$$\mathrm{NTTC} = \mathrm{UNTTF} \times \mathrm{INTTR} \tag{53}$$

The formula for calculating intracellular nutrient transfer/transport efficiency (INTTE) is as follows:

$$\mathrm{INTTE} = \frac{1}{\mathrm{UATTF} + \mathrm{UPTTF}} = \frac{\mathrm{IXc}\,\mathrm{IXl}}{\mathrm{IR}(\mathrm{IXc} + \mathrm{IXl})} \tag{54}$$

The calculation formula for the ratio of intracellular active to passive transfer/transport capacity (RAP) is as follows:

$$\mathrm{RAP} = \frac{\mathrm{UATTF}}{\mathrm{UPTTF}} = \frac{\mathrm{IXc}}{\mathrm{IXl}} \tag{55}$$

(4) Dielectric substance transfer/transport capacity

The intracellular dielectric substance transfer/transport capacity of earlobe cells encompasses the transfer quantities of various intracellular dielectric substances, transfer/transport conductance and resistance of different dielectric substances, transfer/transport capacity of various dielectric substances, and transfer/transport ratio of capacitance/inductance-based dielectric substances ($\mathrm{RTTC}_{C\text{-}L}$).

(*i*) *The transfer quantities of diverse intracellular dielectric substances*

The transfer quantities of various intracellular dielectric substances within the cell encompass the transfer number of dielectric substances for response resistance (Kn_R), transfer number of dielectric substances for response impedance (Kn_Z), transfer number of dielectric substances for response capacitive reactance (Kn_{Xc}), and transfer number of dielectric substances for response inductive reactance (Kn_{Xl}).

According to the derivation from Equations (15) and (16), the calculation of the transfer number of dielectric substances for the response resistance (Kn_R) is as follows:

$$\mathrm{Kn}_R = \ln k_1 - \ln y_1 \tag{56}$$

Similarly, the calculations of the transfer number of dielectric substances for response impedance (Kn_Z), the transfer number of dielectric substances for response capacitive reactance (Kn_{Xc}), and the transfer number of dielectric substances for response inductive reactance (Kn_{Xl}) are presented in Equations (57), (58), and (59), respectively.

$$\mathrm{Kn}_Z = \ln k_2 - \ln y_2 \tag{57}$$

$$\mathrm{Kn}_{Xc} = \ln k_3 - \ln y_3 \tag{58}$$

$$\mathrm{Kn}_{Xl} = \ln k_4 - \ln y_4 \tag{59}$$

(*ii*) *The transport conductance and resistance of different dielectric substances*

The transport conductance and resistance of different dielectric substances include the conductive force of resistance-based dielectric substances

(ICF_R), conductive resistance of resistance-based dielectric substances (ICR_R), conductive force of capacitance-based dielectric substances (ICF_C), conductive resistance of capacitance-based dielectric substances (ICR_C), conductive force of inductance-based dielectric substances (ICF_L), conductive resistance of inductance-based dielectric substances (ICR_L), conductive force of impedance-based dielectric substances (ICF_Z) and conductive resistance of impedance-based dielectric substances (ICR_Z).

According to Ohm's law, the current $I = U/R$, where U is the measured voltage (1.5 V) and I is the physiological current. Therefore,

$$I = \frac{1.5}{y_1 + k_1 e^{-b_1 F}} \tag{60}$$

where I is the physiological current, with a measured voltage of 1.5 V. Taking the derivative of the above formula yields

$$I' = \frac{1.5\, b_1 k_1 e^{-b_1 F}}{\left(y_1 + k_1 e^{-b_1 F}\right)^2} \tag{61}$$

Physiological currents are produced by the movement of dielectric substances (comprising inorganic and organic ions) within earlobe cells. This physiological current reflects the conductivity of dielectric substances and is directly related to the conductivity of dielectric substances. The biological significance of the conduction ability based on the physiological current can be characterized by the variation of the physiological current under unit pressure, which represents the conductivity of earlobe cells. Based on Equation (61), when $F = 0$, the conductive force of the resistance-based dielectric substances (ICF_R) is derived as follows:

$$\mathrm{ICF}_R = \frac{1.5\, b_1 k_1}{\left(y_1 + k_1\right)^2} \tag{62}$$

Similar to ICF_R, the conductive forces of capacitance-based dielectric substances (ICF_C), inductance-based dielectric substances (ICF_L), and impedance-based dielectric substances (ICF_Z) were derived:

$$\mathrm{ICF}_C = \frac{1.5\, b_3 k_3}{\left(y_3 + k_3\right)^2} \tag{63}$$

$$\mathrm{ICF}_L = \frac{1.5\, b_4 k_4}{\left(y_4 + k_4\right)^2} \tag{64}$$

$$\mathrm{ICF}_Z = \frac{1.5\, b_2 k_2}{\left(y_2 + k_2\right)^2} \tag{65}$$

Based on the relationship between the resistance and clamping force (Equation (16)), the derivative formula is as follows:

$$R' = -b_1 k_1 e^{-b_1 F} \tag{66}$$

Physiological resistance is the resistance of a system to physiological currents. The biological significance of Equation (66) can be described as the alteration in physiological resistance under unit pressure, signifying the conductive resistance grounded in physiological resistance. When $F = 0$, Equation (66) can be expressed as

$$R'_{F=0} = -b_1 k_1 \tag{67}$$

where $R'_{F=0}$ denotes the intrinsic conductive resistance of earlobe tissue grounded in physiological resistance, specifically, the conductive resistance of resistance-based dielectric substances (ICR_R).

Similar to ICR_R, the conductive resistance of capacitance-based dielectric substances (ICR_C), the conductive resistance of inductance-based dielectric substances (ICR_L), and the conductive resistance of impedance-based dielectric substances (ICR_Z) were derived:

$$\mathrm{ICR}_C = -b_3 k_3 \tag{68}$$

$$\mathrm{ICR}_L = -b_4 k_4 \tag{69}$$

$$\mathrm{ICR}_Z = -b_2 k_2 \tag{70}$$

(*iii*) *The transfer/transport capacity of various dielectric substances*

According to mechanics principles, the acceleration of a substance is directly proportional to its force and inversely proportional to its mass. Therefore, we can define the transfer/transport capacity of resistance-based dielectric substances as $\mathrm{TTC}_R = \mathrm{ICF}_R/\mathrm{Kn}_R$, that of capacitance-based dielectric substances as $\mathrm{TTC}_C = \mathrm{ICF}_C/\mathrm{Kn}_{Xc}$, that of inductance-based dielectric substances as $\mathrm{TTC}_L = \mathrm{ICF}_L/\mathrm{Kn}_{Xl}$, and that of impedance-based dielectric substances as $\mathrm{TTC}_Z = \mathrm{ICF}_Z/\mathrm{Kn}_Z$.

(*iv*) *The transfer/transport ratio of capacitance/inductance-based dielectric substances* ($\mathrm{RTTC}_{C\text{-}L}$)

The transfer/transport ratio of capacitance/inductance-based dielectric substances ($\mathrm{RTTC}_{C\text{-}L}$) is calculated as follows:

$$\mathrm{RTTC}_{C\text{-}L} = \frac{\mathrm{TTC}_C}{\mathrm{TTC}_L} \tag{71}$$

Table 1. Earlobe specific effective thickness and resting electrical parameters of three healthy subjects.

Parameter	Sample 1	Sample 2	Sample 3
Earlobe specific effective thickness (d)	372.25	315.57	183.17
Resting resistance (IR, MΩ)	1.130	1.765	3.605
Resting impedance (IZ, MΩ)	0.286	0.273	0.443
Resting capacitive reactance (IXc, MΩ)	0.328	0.316	0.494
Resting inductive reactance (IXl, MΩ)	2.303	6.340	12.182
Resting capacitance (ICP, pF)	161.76	167.69	107.40
Unit resting resistance (IR_U, MΩ)	420.643	556.981	660.328
Unit resting impedance (IZ_U, MΩ)	106.464	86.151	81.144
Unit resting capacitive reactance (IXc_U, MΩ)	122.098	99.720	90.486
Unit resting inductive reactance (IXl_U, MΩ)	857.292	2000.714	2231.377
Unit resting capacitance (ICP_U, pF)	0.43	0.53	0.59

(5) Metabolic capacity

Metabolic capacity is correlated with bioelectric currents. Higher bioelectric currents indicate greater metabolic capacity. The earlobe resting resistance-based bioelectric current (I_R) is defined as $I_R = U/\mathrm{IR}$; the earlobe resting capacitive reactance-based bioelectric current (I_{Xc}) as $I_{Xc} = U/\mathrm{IXc}$; the earlobe resting inductive reactance-based bioelectric current (I_{Xl}) as $I_{Xl} = U/\mathrm{IXl}$; and the earlobe resting impedance-based bioelectric current (I_{IZ}) as $I_{IZ} = U/\mathrm{IZ}$. Here, U represents the voltage applied during measurement. Because the circuits are parallel, the voltage U remains constant; therefore, we can define the metabolic flux (MF) of the earlobe cells as follows:

$$\mathrm{MF} = \frac{10^5}{\mathrm{IR} \times \mathrm{IZ} \times \mathrm{IXc} \times \mathrm{IXl}} \tag{72}$$

The metabolic strength (MS) of cells can be defined as the natural logarithm of MF, representing the internal energy-driven metabolic strength, calculated as follows:

$$\mathrm{MS} = \ln(\mathrm{MF}) \tag{73}$$

The active nutrient transfer/transport capacity is correlated with the metabolic rate. A stronger active nutrient transfer/transport capacity indicates a higher metabolic rate. Therefore, the metabolic rate (MR) of earlobe cells was defined as follows:

$$\mathrm{MR} = \mathrm{INTTR} \times \mathrm{NATTC} \tag{74}$$

Based on the metabolic flux (MF) and metabolic rate (MR) of earlobe cells, the relative metabolic activity (MA) of the earlobe was defined as follows:

$$\mathrm{MA} = \sqrt[6]{\mathrm{MF} \times \mathrm{MR}} \tag{75}$$

Therefore, the basal metabolic activity (MB) of the earlobe was defined as follows:

$$\mathrm{MB} = \frac{\mathrm{MA}}{d} \tag{76}$$

3 Results

3.1 Pressure-Dependent Model Fitting Accuracy

The coefficients of determination (R^2) of the pressure-dependent models for all earlobe electrical parameters, as computed by the Plant Life Analyzer, were higher than 0.97 ($n = 90$, $P < 0.001$). This indicates that the linear model (capacitance) and the nonlinear exponential decrease models (resistance/impedance/capacitive reactance/inductive reactance) can effectively characterize the dynamic changes of earlobe electrical signals with clamping pressure. The high fitting accuracy supports the applicability of the biophysical models established in this study, and indicates a close correlation between mechanical pressure stimulation and the electrical characteristics of earlobe tissue.

3.2 Earlobe Resting Electrical Parameters

Table 1 presents the earlobe specific effective thickness and resting electrical parameters of the three healthy subjects. The earlobe specific effective thickness d varied among subjects (Sample 1: 372.25, Sample 2: 315.57, Sample 3: 183.17), with Sample 3 showing the smallest d (body composition was

not measured in this study, so leanness is only a hypothesis). Corresponding to the tissue thickness difference, Sample 3 exhibited higher resting resistance (3.605 MΩ) and inductive reactance (12.182 MΩ), but lower resting capacitance (107.40 pF) compared to Samples 1 and 2. The unit resting capacitance (ICP_U) was the highest in Sample 3 (0.59 pF) and ranged from 0.43 to 0.59 pF among the three subjects, so its stability as an intrinsic characteristic of earlobe cells requires confirmation in larger cohorts.

3.3 Energy Conversion Capacity

Table 2 presents the energy conversion capacity biophysical indicators of the three subjects. The average unit internal energy (ΔG_U) ranged from 4.451 to 4.681 across subjects, with consistent values of unit internal energy indicators ($\Delta G_{R\text{-}U}$, $\Delta G_{Z\text{-}U}$, $\Delta G_{Xc\text{-}U}$, $\Delta G_{Xl\text{-}U}$), indicating that healthy subjects had similar cellular energy conversion efficiency (normalized by tissue thickness). The $\mathrm{RG}_{Xc\text{-}Xl}$ ratio–the proposed biophysical biomarker for TCM Yin-Yang balance–was close to 1 (0.986–1.036) in all three subjects, consistent with a balanced physiological and energy conversion status.

Total internal energy indicators (e.g., ΔG_R, ΔG_Z, ΔG_{Xc}, ΔG_{Xl}) were lower in Sample 3 compared to Samples 1 and 2, which was directly attributed to the smaller earlobe specific effective thickness d in Sample 3 (total internal energy = unit internal energy $\times$ d). This result suggests that total internal energy was affected by tissue volume, while unit internal energy was a more stable biophysical indicator for characterizing intrinsic cellular energy metabolism function.

3.4 Intracellular Water and Nutrient Transfer/Transport Capacity

Table 3 presents the intracellular water/nutrient transport capacity biophysical indicators of the three subjects. Sample 3 showed lower intracellular water-holding capacity (IWHC: 1112.949) and water transport rate (IWTTR: 23.416) compared to Samples 1 and 2, which was associated with the smaller earlobe tissue thickness and lower intracellular water content in Sample 3. The intracellular water transport efficiency (IWTTE) was similar among the three subjects, indicating consistent water transport efficiency per unit tissue thickness in healthy subjects.

For nutrient transport capacity, Sample 3 exhibited lower active nutrient transfer/transport capacity (NATTC: 6.929) compared to Samples 1 and 2, whereas passive nutrient transfer/transport capacity (NPTTC) was comparable between Samples 1 and 3 and highest in Sample 2. The ratio of active to passive nutrient transfer/transport (RAP) was the lowest in Sample 3 (0.041), indicating a predominance of passive nutrient transport in Sample 3, which may be a compensatory biophysical mechanism for reduced active transport capacity. The total nutrient transfer/transport capacity (NTTC) was similar in Samples 1 and 3 but higher in Sample 2, suggesting that the reduced active transport in Sample 3 was largely offset by passive transport.

3.5 Dielectric Substance Transfer Capacity

Table 4 presents the dielectric substance transfer capacity biophysical indicators of the three subjects. The transfer number of dielectric substances (Kn_R, Kn_Z, Kn_{Xc}, Kn_{Xl}) was consistent among the three subjects, indicating that healthy subjects had similar dielectric substance transfer efficiency in earlobe cells. Sample 3 had lower conductive force (ICF_R: 0.273 vs. 1.027 and 0.579; ICF_C: 1.526 vs. 2.655 and 2.497; ICF_L: 0.111 vs. 0.538 and 0.221; ICF_Z: 1.672 vs. 3.151 and 2.822) and transfer/transport capacity (TTC_R: 0.082 vs. 0.291 and 0.174; TTC_C: 0.604 vs. 0.965 and 0.964; TTC_L: 0.027 vs. 0.141 and 0.053; TTC_Z: 0.671 vs. 1.123 and 1.109). The $\mathrm{RTTC}_{C\text{-}L}$ ratio was higher in Sample 3 (22.434), reflecting a relative increase in capacitance-based dielectric substance transfer/transport in Sample 3.

3.6 Metabolic Capacity

For metabolic capacity biophysical indicators (Table 5), Sample 3 exhibited lower metabolic flux (MF), metabolic rate (MR), and metabolic activity (MA) compared to Samples 1 and 2 (e.g., MF: 10.407×10^3 vs. 409.499×10^3 and 103.314×10^3; MR: 162.258 vs. 970.440 and 624.812; MA: 10.915 vs. 27.116 and 20.030). The basal metabolic activity (MB)–a normalized metabolic capacity indicator (MA/d)–was slightly lower in Sample 3 (0.060) and consistent among healthy subjects, indicating that the intrinsic metabolic activity per unit tissue thickness was stable in healthy human bodies, and the lower total metabolic capacity in Sample 3 was due to reduced tissue volume. All metabolic capacity indicators varied in parallel with water/nutrient transfer/transport capacity, consistent with an inherent biophysical link between earlobe electrical characteristics, substance transfer/transport and cellular metabolic function.

Table 2. Energy conversion capacity biophysical indicators of three healthy subjects.

Parameter	Sample 1	Sample 2	Sample 3
Resistance-based unit internal energy ($\Delta G_{R\text{-}U}$)	4.425	4.730	4.889
Capacitive reactance-based unit internal energy ($\Delta G_{Xc\text{-}U}$)	4.454	4.575	4.656
Impedance-based unit internal energy ($\Delta G_{Z\text{-}U}$)	4.406	4.587	4.666
Inductive reactance-based unit internal energy ($\Delta G_{Xl\text{-}U}$)	4.518	4.416	4.514
Average unit internal energy (ΔG_U)	4.451	4.577	4.681
Capacitive reactance internal energy/inductive reactance internal energy ($\mathrm{RG}_{Xc\text{-}Xl}$)	0.986	1.036	1.031
Resistance-based internal energy (ΔG_R)	1647.117	1492.538	895.467
Impedance-based internal energy (ΔG_Z)	1640.073	1447.392	854.702
Capacitive reactance-based internal energy (ΔG_{Xc})	1657.858	1443.689	852.831
Inductive reactance-based internal energy (ΔG_{Xl})	1681.889	1393.688	826.791

Table 3. Water and nutrient transfer/transport capacity biophysical indicators.

Parameter	Sample 1	Sample 2	Sample 3
Intracellular water-holding capacity (IWHC)	2057.362	2171.574	1112.949
Intracellular water-holding time (IWHT)	46.268	45.843	47.529
Intracellular water transfer/transport efficiency (IWTTE)	0.181	0.145	0.165
Intracellular water/nutrient transfer/transport rate (IWTTR/INTTR)	44.466	47.369	23.416
Intracellular nutrient transfer/transport efficiency (INTTE)	0.254	0.171	0.132
Active transfer/transport unit flow (UATTF)	0.491	0.278	0.296
Intracellular nutrient active transfer/transport capacity (NATTC)	21.824	13.190	6.929
Intracellular nutrient passive transfer/transport unit flow (UPTTF)	3.446	5.581	7.298
Intracellular nutrient passive transfer/transport capacity (NPTTC)	153.255	264.327	170.874
Intracellular nutrient transfer/transport unit flow (UNTTF)	3.937	5.859	7.594
Intracellular nutrient transfer/transport capacity (NTTC)	175.079	277.517	177.803
Ratio of intracellular active to passive transfer/transport capacity (RAP)	0.142	0.050	0.041

4 Discussion

4.1 Biophysical Mechanisms of Earlobe Electrical Signals Reflecting Systemic Physiological Function

The earlobe, a peripheral tissue characterized by a homogeneous adipofibrous structure and rich microcirculation, is a readily accessible site whose morphological changes (e.g., ear lobe crease) have been associated with systemic disease such as coronary artery disease [11]. Its electrical characteristics are intrinsically associated with cell membrane permeability, transmembrane ion gradient dynamics, intracellular substance concentration homeostasis, and basal metabolic activity. For example, capacitance is primarily determined by the phospholipid bilayer structure of the cell membrane and intracellular water content [12], whereas, in the plant electrophysiological framework on which this method is based, resistance and impedance reflect intracellular water and salt (ion) transfer/transport [8].

In this study, the established pressure-dependent biophysical models achieved high fitting accuracy ($R^2 > 0.97$), indicating a close biophysical correlation between mechanical clamping pressure and earlobe electrical signal changes. The underlying mechanism is that clamping pressure alters the volume and microcirculation of earlobe tissue, leading to changes in intracellular water content and ion transport–both of which directly affect the dielectric and conductive properties of the tissue, and thus the measured electrical parameters.

Notably, the inter-sample variability of earlobe electrical parameters and derived physiological indicators appeared lower than that reported for plant leaf electrophysiological measurements obtained

Table 4. Dielectric substance transfer capacity biophysical indicators.

Parameter	Sample 1	Sample 2	Sample 3
Transfer number of dielectric substances for response resistance (Kn_R)	3.524	3.337	3.327
Transfer number of dielectric substances for response capacitive reactance (Kn_{Xc})	2.750	2.590	2.526
Transfer number of dielectric substances for response inductive reactance (Kn_{Xl})	3.817	4.184	4.122
Transfer number of dielectric substances for response impedance (Kn_Z)	2.807	2.544	2.492
Conductive force of resistance-based dielectric substances (ICF_R)	1.027	0.579	0.273
Conductive force of capacitance-based dielectric substances (ICF_C)	2.655	2.497	1.526
Conductive force of inductance-based dielectric substances (ICF_L)	0.538	0.221	0.111
Conductive force of impedance-based dielectric substances (ICF_Z)	3.151	2.822	1.672
Conductive resistance of resistance-based dielectric substances (ICR_R)	-0.874	-1.203	-2.368
Conductive resistance of capacitance-based dielectric substances (ICR_C)	-0.190	-0.167	-0.248
Conductive resistance of inductance-based dielectric substances (ICR_L)	-1.904	-5.916	-10.946
Conductive resistance of impedance-based dielectric substances (ICR_Z)	-0.172	-0.141	-0.218
Transfer/transport capacity of resistance-based dielectric substances (TTC_R)	0.291	0.174	0.082
Transfer/transport capacity of capacitance-based dielectric substances (TTC_C)	0.965	0.964	0.604
Transfer/transport capacity of inductance-based dielectric substances (TTC_L)	0.141	0.053	0.027
Transfer/transport capacity of impedance-based dielectric substances (TTC_Z)	1.123	1.109	0.671
Transfer/transport ratio of capacitance/inductance-based dielectric substances ($\mathrm{RTTC}_{C\text{-}L}$)	6.850	18.252	22.434

Table 5. Metabolic capacity biophysical indicators.

Parameter	S1	S2	S3
Metabolic flux (MF, $\times 10^3$)	409.499	103.314	10.407
Metabolic strength (MS)	12.920	11.546	9.250
Metabolic rate (MR)	970.440	624.812	162.258
Metabolic activity (MA)	27.116	20.030	10.915
Basal metabolic activity (MB)	0.073	0.064	0.060

with the same measurement principle [13]. This difference may be ascribed to two biological and experimental characteristics. First, human earlobe cells lack cell walls and exhibit high structural homogeneity. Conversely, plant leaf cells have a heterogeneous tissue composition (including epidermis, mesophyll, and veins) and rigid cell walls, which result in substantial inter-sample differences in the acquisition of electrical signals. Second, the electrophysiological parameters of plant leaves respond to external environmental conditions such as salinity stress and physiological adaptation [13]. In contrast, human earlobe tissue, as a closed peripheral tissue, maintains a relatively stable internal microenvironment, thus minimizing nonphysiological variability. Additionally, all participants in this study were healthy adult males of similar age (approximately 63 years), which further reduced the inherent physiological variability compared to plant studies involving different growth stages and environmental exposures. The reduced inter-sample variability makes the earlobe electrical

parameters a more stable and reproducible biomarker for evaluating human physiological status than the plant leaf parameters.

Sample 3, the participant with the smallest earlobe thickness among the three healthy participants (possibly a leaner subject, although body composition was not measured), demonstrated distinct electrical and physiological features: a smaller earlobe thickness (183.17 compared to 372.25 and 315.57), a higher resting resistance and inductive reactance, a lower resting capacitance, and decreased rates of water/nutrient transfer/transport as well as metabolic activity. This suggests that body composition (e.g., proportion of lean mass), which was not measured here, might be a significant confounding factor in earlobe electrical parameter measurements. Lean individuals generally possess less adipose tissue in the earlobe, which directly influences tissue thickness and cellular density, the key determinants of electrical signal propagation, and capacitance/resistance characteristics.

4.2 Potential Correlation between Earlobe Biophysical Information and Visceral Function

The quantified biophysical indicators derived from earlobe electrical parameters exhibit potential correlations with the functional states of multiple human visceral organs and pathogenesis of prevalent chronic diseases. This suggests a noninvasive link between peripheral tissue electrical signals and systemic organ function. Notably, the distinctive characteristics of Sample 3 provide preliminary insights into how physiological disparities associated with body composition may correspond to organ function and disease risk.

The energy conversion capacity of unit tissue cells ($\Delta G_{R\text{-}U}$, $\Delta G_{Xc\text{-}U}$, $\Delta G_{Xl\text{-}U}$, $\Delta G_{Z\text{-}U}$, and $\mathrm{RG}_{Xc\text{-}Xl}$) is closely correlated with the mitochondrial respiratory function, which serves as the core of cellular energy metabolism. The energy conversion capacity of unit tissue cells in the three healthy males demonstrated comparable values, suggesting similar mitochondrial function. Nevertheless, lower values may imply decreased mitochondrial activity and diminished basal metabolism. Clinically, impaired mitochondrial energy conversion is a recognized pathological feature of myocardial dysfunction, where mitochondrial impairment reduces cardiac energy supply and contractile function in heart failure [14]. An $\mathrm{RG}_{Xc\text{-}Xl}$ ratio approaching 1 (0.986–1.036) in all samples indicates balanced energy conversion, which is consistent with their healthy state; deviations from this ratio may signify imbalanced energy metabolism, a prevalent precursor of metabolic syndrome and endocrine disorders (e.g., thyroid dysfunction) [15]. These proposed associations should be interpreted with caution and require independent clinical validation in larger, more diverse cohorts.

The IWHC and IWTTR reflect intracellular water content and its transmembrane transport. The comparatively lower values of IWHC and IWTTR in Sample 3 (1112.949 in contrast to 2057.362 and 2171.574; 23.416 in contrast to 44.466 and 47.369) may imply a reduction in the intracellular water content in Sample 3. This finding is in accordance with the lower amount of adipose tissue (a tissue component that may influence water content); however, it might also coincide with differences in renal tubular function, whose dysfunction is linked to adverse kidney outcomes [16].

NATTC, mediated by cellular transport proteins, is associated with intestinal nutrient absorption and pancreatic islet function. The decline in NATTC in Sample 3 (6.929, compared to 21.824 and 13.190) may indicate a reduction in the active transport of amino acids and other nutrients, which depends on intestinal and renal epithelial transporters [17]. RAP was lowest in Sample 3 (0.041, as opposed to 0.142 and 0.050), suggesting a predominance of passive nutrient transfer. This could serve as a compensatory mechanism for the decreased active transfer/transport in Sample 3.

The similar transfer numbers of diverse types of intracellular dielectric substances (Kn_R, Kn_Z, Kn_{Xc}, and Kn_{Xl}) suggested comparable efficiencies in the transfer/transport of inorganic ions and organic molecules among the three samples. The conductive force of dielectric substances (ICF_R, ICF_C, ICF_L, and ICF_Z) and transfer/transport capacity (TTC_R, TTC_C, TTC_L, and TTC_Z) reflect the intensity of transmembrane ion and organic molecule transport, which are intricately linked to cardiovascular function [18]. The lower ICF_R (0.273 vs. 1.027 and 0.579) and TTC_R (0.082 vs. 0.291 and 0.174) of Sample 3 imply a decrease in ion transport quantity, which may be related to blood volume or cardiac output (not measured here). Clinically, impaired ion transport (e.g., Na^+, K^+, and Ca^{2+}) represents a core pathological mechanism of hypertension and arrhythmia [19]; hence, these parameters may potentially serve as early biomarkers for cardiovascular risk stratification. Furthermore, a reduction in

dielectric substance transfer and conveyance capacity may reflect impaired transmembrane ion transport, which is a plausible but untested link to peripheral tissue conductivity changes in this cohort.

MA and MB function as comprehensive indices of systemic metabolic activity. The lower MA (10.915 compared to 27.116 and 20.030) and MB (0.060 compared to 0.073 and 0.064) values in Sample 3 coincided with low intracellular water and nutrient transfer/transport efficiency, low active transfer/transport capacity, and diminished conductive force. Clinically, diminished metabolic capacity is a characteristic feature of obesity, hypothyroidism, and chronic kidney disease, all of which are characterized by systemic metabolic suppression [20, 21]. The MR and MF in Sample 3 were also notably lower, which might represent a physiological adaptation to the reduction in adipose tissue stores and energy reserves.

4.3 Advantages of the Established Non-Invasive Biophysical Detection Method

Compared with conventional physiological assessment methods, the non-invasive biophysical detection method established in this study based on earlobe electrical parameters and pressure-dependent models exhibits potential biophysical and clinical advantages, especially for large-scale health screening and on-site physiological assessment:

4.3.1 Non-invasiveness, Safety, and Repeatability

This approach employs a clamp-on parallel-plate capacitor sensor integrated into a portable Plant Life Analyzer, enabling the acquisition of electrical signals without the need for blood sampling, puncture, or other invasive procedures. This eliminates the risk of infection and mitigates patient discomfort, making it suitable for repetitive measurements during long-term health monitoring and large-scale screening.

4.3.2 Portability and Field Applicability

This portable device allows on-site measurements in primary care clinics, community health centers, and mobile screening scenarios. The entire detection process (excluding the 20-min rest period) takes $<$ 3 min, meeting rapid health assessment needs.

4.3.3 Comprehensiveness and Holism

Unlike single-index detection methods (e.g., blood glucose, lipid analysis), this method quantifies multiple interrelated biophysical processes (energy conversion, water/nutrient transport, dielectric substance transfer, metabolic capacity) from a single set of earlobe electrical signals, providing a comprehensive biophysical assessment of systemic physiological function. This is particularly important for sub-health identification and early disease detection, where single biomarkers may be insensitive.

4.3.4 Integration of TCM and Western Medicine

The $\mathrm{RG}_{Xc\text{-}Xl}$ ratio, derived from the internal energy of capacitive and inductive reactance, is proposed here as a candidate quantitative biophysical index for TCM's "Yin-Yang balance" concept, which has previously been related to the balance between oxidation and antioxidation processes [22]. This interpretation may help narrow the gap between the qualitative holistic diagnosis in TCM and quantitative molecular diagnosis in Western medicine, and could support the modernization and quantification of TCM theory in clinical applications. However, this interpretation remains a hypothesis that requires independent clinical validation before the ratio can be considered an established physiological biomarker.

4.4 Study Limitations and Future Research Directions

This study establishes a pressure-dependent biophysical model for earlobe electrical parameters and examines its feasibility for non-invasive physiological assessment, but has several limitations that need to be addressed in future research: (1) The study is a pilot biophysical modeling study with a small sample size, and no repeated test sessions (e.g., on different days) were performed for each participant–future research will expand the sample size to include diverse age groups, genders and body compositions, and conduct test-retest measurements to further verify the stability and repeatability of the biophysical models; (2) The study focuses on healthy subjects, with no validation in patients with chronic diseases (e.g., diabetes, hypertension, liver disease)–the correlation between earlobe electrical parameters and disease-specific biophysical changes remains to be explored; (3) The portable detection system needs further optimization to adapt to diverse earlobe sizes (especially extremely thin/thick earlobes) and reduce measurement errors from tissue compression variability; (4) The biophysical mechanisms linking earlobe electrical parameters with systemic visceral organ function need to be further elucidated through in-depth cellular and molecular biological research.

Future research will focus on the following

directions to enhance the scientific rigor and clinical applicability of the method: (1) Expand and diversify the research sample to optimize the pressure-dependent biophysical models and establish body composition-specific reference ranges of biophysical indicators; (2) Conduct case-control studies in chronic disease patients to identify disease-specific earlobe electrical signal patterns and establish diagnostic cut-off values for early disease detection; (3) Optimize the portable biophysical detection system with real-time pressure feedback and automatic earlobe thickness calibration to reduce measurement errors and improve adaptability; (4) Elucidate the underlying biophysical mechanisms between earlobe electrical parameters and systemic physiological function, and explore the correlation between earlobe biophysical indicators and gold-standard clinical physiological parameters; (5) Integrate machine learning algorithms with earlobe electrical signal analysis to develop an intelligent biophysical assessment system for large-scale health screening and personalized health management; (6) Explore the therapeutic application of earlobe electrical signals, which may provide the basic electrical signals for future electronically controlled treatment of diseases, thereby extending the method's application from non-invasive physiological assessment to therapeutic intervention.

5 Conclusion

This study presents a non-invasive biophysical detection method for rapid quantification of human systemic physiological information via earlobe electrical parameters, and establishes a pressure-dependent biophysical model (linear for capacitance, nonlinear exponential for $R/Z/Xc/Xl$) based on the Gibbs free energy equation and Nernst equation. The biophysical models achieve high fitting accuracy ($R^2 > 0.97$), and key biophysical indicators (energy conversion capacity, water/nutrient transfer/transport capacity, dielectric substance transfer capacity, metabolic capacity) are derived to characterize human systemic physiological function.

The experimental results support the feasibility of the established method and models: (1) Healthy subjects exhibit similar transfer numbers of dielectric substances, water transport efficiency, and unit internal energy, whereas other normalized indicators (e.g., unit resting resistance and inductive reactance) differed markedly among the three subjects, so the stability of the method requires verification in larger cohorts; (2) The $\mathrm{RG}_{Xc\text{-}Xl}$ ratio (0.986–1.036) is proposed as a candidate quantitative biophysical biomarker for TCM Yin-Yang balance, providing an objective biophysical indicator for holistic physiological health assessment; (3) Body composition (e.g., leanness), which was not measured here, may be a factor influencing earlobe electrical parameters and derived biophysical indicators, and normalizing parameters by tissue thickness reduces individual differences; (4) The custom portable detection system enables rapid on-site biophysical detection (total time < 3 min), making the method suitable for large-scale health screening and primary healthcare.

This study indicates that earlobe electrical parameters can serve as a sensitive peripheral biophysical signature of human systemic physiological function. The established non-invasive, portable biophysical detection method may help connect TCM holistic theory with Western quantitative biophysical modeling, and provides a new biophysical tool for non-invasive physiological assessment. The method has potential theoretical and clinical value, with possible applications in public health screening, early disease detection, TCM modernization and personalized health management. The quantifiable earlobe electrical signals may also provide the basic electrical signals for future electronically controlled treatment of diseases, opening a therapeutic application avenue beyond physiological assessment. Future research will expand the sample size, validate the method in disease populations, and optimize the detection system to further enhance its clinical utility.

Abbreviations: TCM, Traditional Chinese Medicine; C_p, Capacitance; R, Resistance; Z, Impedance; Xc, Capacitive reactance; Xl, Inductive reactance; d, Earlobe specific effective thickness; IR, Resting resistance; IZ, Resting impedance; IXc, Resting capacitive reactance; IXl, Resting inductive reactance; ICP, Resting capacitance; IR_U, Unit resting resistance; IZ_U, Unit resting impedance; IXc_U, Unit resting capacitive reactance; IXl_U, Unit resting inductive reactance; ICP_U, Unit resting capacitance; $\Delta G_{R\text{-}U}$, Resistance-based unit internal energy; $\Delta G_{Z\text{-}U}$, Impedance-based unit internal energy; $\Delta G_{Xc\text{-}U}$, Capacitive reactance-based unit internal energy; $\Delta G_{Xl\text{-}U}$, Inductive reactance-based unit internal energy; ΔG_U, Average unit internal energy; $\mathrm{RG}_{Xc\text{-}Xl}$, Capacitive reactance internal energy/inductive reactance internal energy; ΔG_R, Resistance-based internal energy; ΔG_Z, Impedance-based internal

energy; ΔG_{Xc}, Capacitive reactance-based internal energy; ΔG_{Xl}, Inductive reactance-based internal energy; IWHC, Intracellular water-holding capacity; IWHT, Intracellular water-holding time; IWTTE, Intracellular water transfer/transport efficiency; IWTTR, Intracellular water transfer/transport rate; INTTR, Intracellular nutrient transfer/transport rate; INTTE, Intracellular nutrient transfer/transport efficiency; UATTF, Active transfer/transport unit flow; NATTC, Intracellular nutrient active transfer/transport capacity; UPTTF, Intracellular nutrient passive transfer/transport unit flow; NPTTC, Intracellular nutrient passive transfer/transport capacity; UNTTF, Intracellular nutrient transfer/transport unit flow; NTTC, Intracellular nutrient transfer/transport capacity; RAP, Ratio of intracellular active to passive transfer/transport capacity; Kn_R, Transfer number of dielectric substances for response resistance; Kn_{Xc}, Transfer number of dielectric substances for response capacitive reactance; Kn_{Xl}, Transfer number of dielectric substances for response inductive reactance; Kn_Z, Transfer number of dielectric substances for response impedance; ICF_R, Conductive force of resistance-based dielectric substances; ICF_C, Conductive force of capacitance-based dielectric substances; ICF_L, Conductive force of inductance-based dielectric substances; ICF_Z, Conductive force of impedance-based dielectric substances; ICR_R, Conductive resistance of resistance-based dielectric substances; ICR_C, Conductive resistance of capacitance-based dielectric substances; ICR_L, Conductive resistance of inductance-based dielectric substances; ICR_Z, Conductive resistance of impedance-based dielectric substances; TTC_R, Transfer/transport capacity of resistance-based dielectric substances; TTC_C, Transfer/transport capacity of capacitance-based dielectric substances; TTC_L, Transfer/transport capacity of inductance-based dielectric substances; TTC_Z, Transfer/transport capacity of impedance-based dielectric substances; $\mathrm{RTTC}_{C\text{-}L}$, Transfer/transport ratio of capacitance/inductance-based dielectric substances; MF, Metabolic flux; MS, Metabolic strength; MR, Metabolic rate; MA, Metabolic activity; MB, Basal metabolic activity.

Data Availability Statement

The data presented in this study are available upon request from the author.

Acknowledgement

The author sincerely thanks the three participants who volunteered for the earlobe electrical parameter measurement experiments for their valuable support. The author also acknowledges the technical support from Jiangsu Zhong-tian Smart Sense Life Data Co., Ltd. for the development and calibration of the portable biophysical detection system (Plant Life Analyzer).

Funding

This work was supported without any funding.

Conflicts of Interest

The authors declare no conflicts of interest.

Author Contributions

All work was conducted by the sole author.

AI Use Statement

The author declares that generative AI (Doubao) was used solely for language translation (Chinese to English) during manuscript preparation. The author reviewed and edited the output and takes full responsibility for the content.

Ethical Approval and Consent to Participate

Ethical review and approval were waived for this study because it involved non-invasive collection of physiological data only (earlobe electrical parameter measurements via a clamp-on sensor without any puncture, blood sampling, or other invasive procedures), with no intervention, no manipulation of the participants' physiological state, and no potential physical, psychological or privacy risks to the healthy adult male participants. All experimental procedures were non-intrusive, and the collected data were anonymized for analysis and reporting, fully complying with the ethical principles of minimal risk research for human subjects. Informed consent was obtained from all the subjects involved in the study.

References

[1] McLamore, E. S., & Porterfield, D. M. (2011). Non-invasive tools for measuring metabolism and biophysical analyte transport: self-referencing physiological sensing. *Chemical Society Reviews*, *40*(11), 5308-5320. [CrossRef]

[2] Northrop, R. B. (2017). *Non-invasive instrumentation and measurement in medical diagnosis* (2nd ed.). CRC Press. [CrossRef]

[3] Zhang, C., Wu, Y., Su, Y., Xing, D., Dai, Y., Wu, Y., & Fang, L. (2020). A plant's electrical parameters indicate its physiological state: A study of intracellular water metabolism. *Plants, 9*(10), 1256. [CrossRef]

[4] Iveson-Iveson, J. (1979). Anatomy and physiology: The ear. *Nursing Mirror, 148*(7), 26-28. https://pubmed.ncbi.nlm.nih.gov/253351/

[5] Langlands, J. H. M., & Wallace, W. F. M. (1965). Small blood-samples from ear-lobe puncture: A substitute for arterial puncture. *The Lancet, 286*(7407), 315-317. [CrossRef]

[6] McKee, T. J., Perlman, G., Morris, M., & Komarova, S. V. (2019). Extracellular matrix composition of connective tissues: a systematic review and meta-analysis. *Scientific Reports, 9*(1), 10542. [CrossRef]

[7] Zhukov, A., & Popov, V. (2023). Eukaryotic cell membranes: Structure, composition, research methods and computational modelling. *International Journal of Molecular Sciences, 24*(13), 11226. [CrossRef]

[8] Wang, J., Wu, Y., Xing, D., Zhang, Q., Quispe Puma, M. R., & Chen, Q. (2025). Dynamic traits of intracellular water and salt based on electrophysiological measurements during adaptations of three mangrove species under salinity stresses. *Horticulturae, 11*(3), 309. [CrossRef]

[9] Mitchell, P. (1961). Coupling of phosphorylation to electron and hydrogen transfer by a chemi-osmotic type of mechanism. *Nature, 191*(4784), 144-148. [CrossRef]

[10] Held, C., & Sadowski, G. (2016). Thermodynamics of bioreactions. *Annual Review of Chemical and Biomolecular Engineering, 7*(1), 395-414. [CrossRef]

[11] Lucenteforte, E., Romoli, M., Zagli, G., Gensini, G. F., Mugelli, A., & Vannacci, A. (2014). Ear lobe crease as a marker of coronary artery disease: a meta-analysis. *International Journal of Cardiology, 175*(1), 171-175. [CrossRef]

[12] Gabriel, C., Gabriel, S., & Corthout, E. (1996). The dielectric properties of biological tissues: I. Literature survey. *Physics in Medicine & Biology, 41*(11), 2231-2249. [CrossRef]

[13] Wang, J., Aboueldahab, M., Wu, Y., Xing, D., & Zhang, Q. (2026). Salt adaptation in *Aegiceras corniculatum*: Electrophysiology, gene expression, and energy trade-offs. *Journal of Plant Electrobiology, 1*(1), 7-31. [CrossRef]

[14] Liu, M., Lv, J., Pan, Z., Wang, D., Zhao, L., & Guo, X. (2022). Mitochondrial dysfunction in heart failure and its therapeutic implications. *Frontiers in Cardiovascular Medicine, 9*, 945142. [CrossRef]

[15] Teixeira, P. F. S., dos Santos, P. B., & Pazos-Moura, C. C. (2020). The role of thyroid hormone in metabolism and metabolic syndrome. *Therapeutic Advances in Endocrinology and Metabolism, 11*, 2042018820917869. [CrossRef]

[16] Bullen, A. L., Fregoso, A., Ascher, S. B., Shlipak, M. G., Ix, J. H., & Rifkin, D. E. (2023). Markers of kidney tubule dysfunction and major adverse kidney events. *Nephron, 147*(12), 713-716. [CrossRef]

[17] Broer, S. (2008). Amino acid transport across mammalian intestinal and renal epithelia. *Physiological Reviews, 88*(1), 249-286. [CrossRef]

[18] Ikeda, Y., Martone, M., Gu, Y., Hoshijima, M., Thor, A., Oh, S. S., ... & Ross Jr, J. (2000). Altered membrane proteins and permeability correlate with cardiac dysfunction in cardiomyopathic hamsters. *American Journal of Physiology-Heart and Circulatory Physiology, 278*(4), H1362-H1370. [CrossRef]

[19] Marazzato, J., Blasi, F., Golino, M., Verdecchia, P., Angeli, F., & De Ponti, R. (2022). Hypertension and arrhythmias: A clinical overview of the pathophysiology-driven management of cardiac arrhythmias in hypertensive patients. *Journal of Cardiovascular Development and Disease, 9*(4), 110. [CrossRef]

[20] Cheng, Y., Hu, H., Li, W., Nie, S., Zhou, S., Chen, Y., ... & Wan, Q. (2025). Chronic kidney disease and thyroid hormones. *The Journal of Clinical Endocrinology & Metabolism, 110*(8), e2446-e2455. [CrossRef]

[21] Yang, M., Liu, S., & Zhang, C. (2022). The related metabolic diseases and treatments of obesity. *Healthcare, 10*(9), 1616. [CrossRef]

[22] Ou, B., Huang, D., Hampsch-Woodill, M., & Flanagan, J. A. (2003). When east meets west: The relationship between yin-yang and antioxidation-oxidation. *The FASEB Journal, 17*(2), 127-129. [CrossRef]



Yanyou Wu holds a Ph.D. in Botany, an M.S. in Plant Physiology and Biochemistry, and a B.S. in Biology. His research focuses on plant biophysics, electrobiology, and environmental adaptation. He has dedicated himself to explaining the fertility of certain intergeneric hybrids through "cell fusion-chromosome set segregation" and the extended genetic laws in his early years. He proposed a new mechanism of photosynthetic oxygen release: half of the oxygen originates from the photolysis of bicarbonate, and the other half from the photolysis of water. He has also innovated plant electrobiological information detection technology and invented a plant life information instrument. Additionally, he created a technical method for characterizing physical information of life (including humans) based on the energy storage and conversion of cellular electrical components. (Email: wuyanyou@mail.gyig.ac.cn)